

# EQUILIBRIUM LENGTH OF A ZENER-BARENBLATT NANOCRACK WEDGED OPEN BY A DISCLINATION DIPOLE

Mao S. Wu

Department of Engineering Mechanics, University of Nebraska-Lincoln,  
Lincoln, NE 68588-0526, USA

## ABSTRACT

The aim of this paper is to investigate the equilibrium length of a stable, mode I nanocrack wedged open by a disclination dipole and subjected to a remote stress. The crack is assumed to be of the Zener type with its head coinciding with the negative disclination of the dipole. Also assumed is the Barenblatt model, in which cohesive zones carrying the theoretical tensile stress exist at the crack extremities. The resulting Zener-Barenblatt crack is modeled by edge dislocations. Exact equations for computing the crack length and cohesive zone lengths are presented. Numerical results show that for a stable nanocrack  $10^{-9}$  to  $10^{-8}$  m in length: (i) the cohesive zones constitute a significant portion of the crack, (ii) the traction-free zone length is significantly less than the predicted length of a purely elastic Zener crack with no cohesive zones, (iii) the traction-free zone length increases with the disclination dipole strength  $\mathbf{w}$  and arm length  $2a$ , and (iv) the cohesive zone at the crack head decreases in length with both  $\mathbf{w}$  and  $2a$  while that at the crack tip increases in length with these parameters.

## KEYWORDS

Zener-Barenblatt crack, disclination dipole, cohesive zones

## 1. INTRODUCTION

Disclinations have been used to model various dislocation ensembles in materials undergoing transformation plasticity, e.g., twinning and strain-induced martensitic transformation. In particular, the front of a deformation twin can be modeled by a wedge disclination dipole [1, 2]. When a twin is blocked by an intersecting twin, a very short crack (nanocrack with length  $10^{-9}$  to  $10^{-8}$  m) can nucleate from the negative disclination of the dipole.

The characteristics of such a nanocrack have only been recently predicted [3]. In this paper, a stable nanocrack subjected to remote mode I loading and wedged open by a disclination dipole is further studied. The wedge-shape crack is modeled as a Zener crack, which is characterized by the crack head opening  $b_T$ . For a very short crack with length 10 – 100 times the Burgers vector magnitude, however, the classical traction-free Zener crack may no longer be physically valid. Consequently, the Barenblatt model is invoked, in which atomistic cohesion exists at the crack extremities. Tractions, which for simplicity are taken to be constant and equal to the theoretical tensile stress, act over these cohesive zones. Of primary interests then are the total length of such a Zener-Barenblatt crack, the cohesive zone lengths, and their dependence on the disclination parameters, i.e., the dipole strength  $\mathbf{w}$  and the dipole arm length  $2a$ . Moreover, it is of interest to

compare the length of the classical (elastic) Zener crack with that of the Zener-Barenblatt (cohesive) crack, thus providing a basis for rejecting or accepting the classical model in lieu of the cohesive model.

The technique of solution relies upon the dislocation modeling of the entire Zener-Barenblatt crack. Exact closed-form expressions have been obtained for the density  $B$  of the modeling edge dislocations, the crack opening displacement  $v$ , and the normal stress  $\mathbf{s}_y = \mathbf{s}$  on the crack line (subscript  $y$  indicates the crack normal direction) [3]. On the basis of exact closed-form expressions for  $v$  and certain consistency relations, the crack length and cohesive zone lengths are computed. These expressions are summarized in Section 2. The numerical results for  $B$ ,  $v$ , the crack length and the cohesive zone lengths are presented in Section 3. A summary of the main findings is given in Section 4.

## 2. EXACT EXPRESSIONS FOR DISCLINATED ZENER-BARENBLATT CRACK

Figure 1 shows the dipole centered at the origin of the  $x$ - $y$  coordinate frame. The negative and positive disclinations of the dipole are located at  $x = -a$  and  $x = a$ , respectively. The strength of each disclination is  $w$ . The crack extends from  $x = a$  to  $x = a + 2c$  on  $y = 0$ . At the crack head  $x = a$ , the opening displacement  $D$  is  $b_T$ . The left cohesive zone is located in the interval  $[a, a + l_1]$ , and the right cohesive zone in  $[a + 2c - l_2, a + 2c]$ . The parameters  $2a$ ,  $2c$ ,  $l_1$  and  $l_2$  denote the dipole arm length, the total crack length, the left and right cohesive zone lengths, respectively. The remote stress  $\mathbf{s}_\infty$  is applied in the direction normal to the crack.

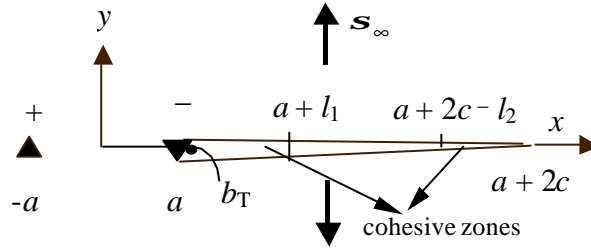


**Figure 1:** A Zener-Barenblatt crack subjected to disclination and remote loadings.

The entire crack is modeled by a continuous distribution of edge dislocations with density  $B(x)$ . As shown by the author in [3],  $B(x)$  is given by:

$$B(x) = \frac{-\sqrt{x-a}\sqrt{a+2c-x}}{p^2 D} \int_a^{a+2c} \frac{\mathbf{s}_d(x') + \mathbf{s}_c(x')}{(x-x')\sqrt{x'-a}\sqrt{a+2c-x'}} dx', \quad (1)$$

where  $D = G/2p(1-\nu)$  ( $G$  is the shear modulus and  $\nu$  the Poisson's ratio),  $\mathbf{s}_d(x')$  is the negative of the sum of remote stress and the  $y$ -component of stress due to the dipole, i.e.:

$$\mathbf{s}_d(x') = -\left( \mathbf{s}_\infty + Dw \ln \left| \frac{a+x'}{a-x'} \right| \right), \quad (2)$$

and  $\mathbf{s}_c(x')$  is the cohesive stress distribution in the intervals  $[a, a + l_1]$  and  $[a + 2c - l_2, a + 2c]$ , i.e.:

$$\mathbf{s}_c(x') = \begin{cases} \mathbf{s}_c \cdot [H(a+l_1) - H(a) + H(a+2c-l_2) - H(a+2c)] \\ \mathbf{s}_c \cdot [-H(a+l_1) + H(a) + H(a+2c-l_2) - H(a+2c)] \end{cases}. \quad (3)$$

In Eqn. (3),  $H$  is the Heaviside function, and the cohesive stress is taken to be the constant  $\mathbf{s}_c$ . Also, the upper expression is used when the left cohesive zone is in compression, while the lower one is used when

the left zone is in tension. The right cohesive zone is always under tension. The left cohesive zone may be under compression or tension since the head of a Zener crack is in compression whereas the negative disclination at the head exerts a tensile stress in this region. Whether the left cohesive zone is in compression or tension is resolved by the sign of the stress intensity factor at  $x = a$  of an elastic Zener crack subjected to the dipole and remote stress loading, see [3]. Substituting Eqns. (2) and (3) into Eqn. (1), a closed-form expression for  $B(x)$  can be obtained. Integrating  $B(x)$  with respect to  $x$  from  $x$  to  $a + 2c$  yields  $v(x)$ , expressible also in closed-form. The crack length  $2c$  and the cohesive zone lengths  $l_1, l_2$  can be determined by equating  $v(x)$  evaluated at  $x = a + 2c - l_2$  to the critical value  $v_{cr}$ , i.e.:

$$\begin{aligned} & \pm \frac{\mathbf{s}_c}{\mathbf{p}^2 D} \left\{ (c-l_1) \ln \left| \frac{c^2 + (c-l_1)(c-l_2) - \sqrt{l_1 l_2 (2c-l_1)(2c-l_2)}}{c(2c-l_1-l_2)} \right| + \right. \\ & \left. (l_2-c) \ln \left| \frac{c^2 + (c-l_1)(c-l_2) + \sqrt{l_1 l_2 (2c-l_1)(2c-l_2)}}{c(2c-l_1-l_2)} \right| + \right. \\ & \left. \sqrt{l_1(2c-l_1)} \left[ -\tan^{-1} \left( \frac{c-l_2}{\sqrt{l_2(2c-l_2)}} \right) + \frac{\mathbf{p}}{2} \right] \right\} + \\ & \frac{\mathbf{s}_c}{\mathbf{p}^2 D} \sqrt{l_2(2c-l_2)} \left\{ -\tan^{-1} \left( \frac{c-l_2}{\sqrt{l_2(2c-l_2)}} \right) + \frac{\mathbf{p}}{2} \right\} + \\ & \frac{2\mathbf{w}}{\mathbf{p}} \left\{ 2\sqrt{a(a+c)} \tan^{-1} \sqrt{\frac{l_2}{2c-l_2}} - (2a+2c-l_2) \tan^{-1} \left( \sqrt{\frac{a}{a+c}} \sqrt{\frac{l_2}{2c-l_2}} \right) \right\} = \Delta_{cr} \end{aligned} \quad (4)$$

and from the following consistency relations (see [3]):

$$\mathbf{s}_c \left\{ \frac{\mathbf{p}}{2} - \tan^{-1} \sqrt{\frac{2c-l_2}{l_2}} \mp \tan^{-1} \sqrt{\frac{l_1}{2c-l_1}} \right\} - \mathbf{p} D \mathbf{w} \tanh^{-1} \sqrt{\frac{a}{a+c}} - \frac{\mathbf{p}}{2} \mathbf{s}_\infty = 0, \quad (5)$$

$$\frac{\mathbf{s}_c}{\mathbf{p} D} \left[ \pm \sqrt{l_1(2c-l_1)} + \sqrt{l_2(2c-l_2)} \right] + 2\mathbf{w} \sqrt{a(a+c)} - a = b_T. \quad (6)$$

The upper and lower signs in Eqns. (4) - (6) correspond to the left cohesive zone being in compression and tension, respectively. These nonlinear equations can be solved numerically for  $c$  and  $l_1, l_2$ . The parameter  $v_{cr}$  equals twice the Burgers vector magnitude  $2b$ . The traction-free crack length  $2x - l_1 - l_2$  can be compared to the crack length  $2c$  of a purely elastic Zener crack (i.e., the classical crack with no cohesive zones).

### 3. NUMERICAL RESULTS

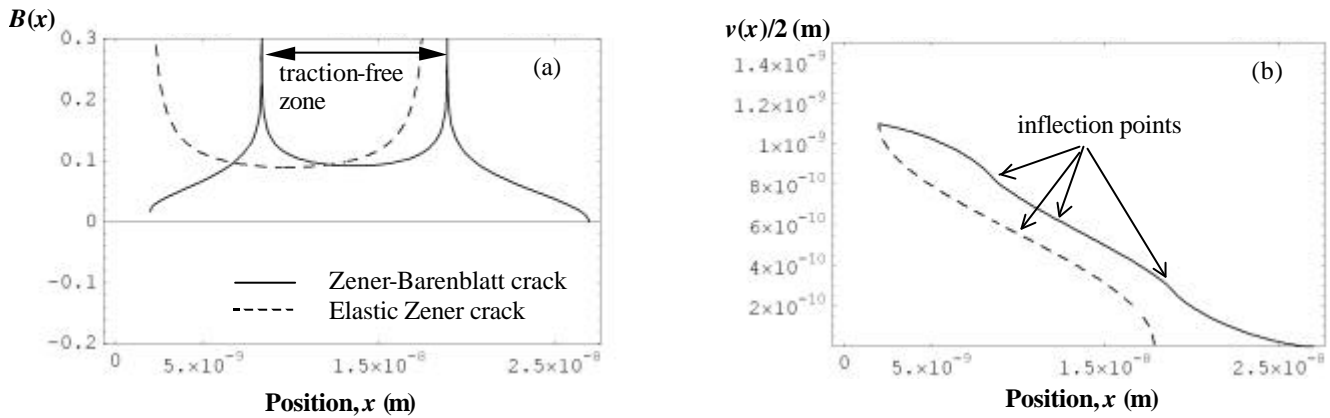
All the numerical results are obtained for the body-centered-cubic metal tungsten (W), except in the last figure where iron (Fe), aluminum (Al), silver (Ag), copper (Cu) and nickel (Ni) are also considered. The parameter  $b$ , taken from [4], and  $\mathbf{g} G, \mathbf{n}$ , taken from [5], are summarized in Table 1. Also listed is the cohesive stress calculated from  $\mathbf{s}_c = 2\mathbf{g}_{cr}$ , where  $\mathbf{g}$  is the crystal-vapor surface energy. For the elastic Zener crack, the crack length is computed by equating the mode I stress intensity factor to the fracture toughness  $K_{IC}$ . The latter is calculated from  $K_{IC} = [4\mathbf{g}G/(1-\mathbf{n})]^{1/2}$ , and the data are also shown in Table 1. Moreover, all numerical results in this paper are generated with  $b_T = 4v_{cr}$  and  $\mathbf{s}_\infty = 0.02$  GPa.

TABLE 1  
MATERIALS DATA (FROM [4, 5])

metals	$b$ $10^{-10}$ m	$g$ $\text{Jm}^{-2}$	$G$ GPa	$n$	$S_c$ GPa	$K_{IC}$ $\text{MPa m}^{-1/2}$
Al	2.8635	0.98	26.5	0.347	3.422	0.399
Ag	2.8894	1.14	33.8	0.354	3.945	0.488
Cu	2.5560	1.725	54.6	0.324	6.749	0.747
Fe	2.4823	1.95	86	0.291	7.856	0.973
Ni	2.4919	2.28	94.7	0.276	9.150	1.092
W	2.7411	2.80	160	0.278	10.21	1.575

### Dislocation Density and Crack Opening Displacement

Figure 2(a) plots  $B(x)$  versus  $x$  for a stable Zener crack wedged open by a dipole of strength  $\mathbf{w} = 1^\circ$  and arm length  $2a = 4$  nm. The solid and dashed lines correspond to the Zener-Barenblatt crack and the elastic Zener crack (crack tips at  $x = a$ , and  $x = 2c$ ), respectively. Also predicted are  $c = 12.5$  nm,  $l_1 = 6.3$  nm,  $l_2 = 8.1$  nm for the former, and  $c = 7.9$  nm for the latter. It can be observed that  $B(x)$  of the Zener-Barenblatt crack is singular at the boundaries between the traction-free zone and the cohesive zones, but is zero at the crack tip  $x = a + 2c$  and has a finite value at the crack head  $x = a$ . These singular points and the minimum point correspond to inflection points on the crack profile. In contrast,  $B(x)$  of the elastic crack is singular at both crack tips. Figure 2(b) plots  $v(x)/2$  versus  $x$ . The Zener-Barenblatt crack has a complex shape with three inflection points as remarked above for Fig. 2(a). It also has a flattened shape at both crack ends. The elastic Zener crack, in contrast, has only one inflection point and has infinite slopes at the ends.



**Figure 2:** (a) Plot of the dislocation densities versus position for the stable Zener-Barenblatt and the elastic Zener cracks. (b) Comparison of the opening displacements of the two cracks.

### Crack Length and Cohesive Zone Lengths

Figure 3 shows the dependence of the traction-free length ( $2c - l_1 - l_2$ ), the total length  $2c$  and the cohesive zone lengths of a stable Zener-Barenblatt crack on  $\mathbf{w}$  and  $a$ . Since  $2c - l_1 - l_2$  is of the order of 50% of  $2c$ , the cohesive zones make up a significant portion of the nanocrack. Second, the traction-free zone length increases with  $\mathbf{w}$  and  $a$ . The total crack length has a more complex dependence on  $\mathbf{w}$  and  $a$ : at the smaller values of  $\mathbf{w}$  and  $a$ ,  $2c$  decreases with increase of these parameters; at the larger values of  $\mathbf{w}$  and  $a$ , the reverse trend is evident. Third, the cohesive zone at the crack head ( $l_1$ ) decreases in length with both  $\mathbf{w}$  and  $a$ , whereas that at the crack tip ( $l_2$ ) increases with these parameters. Fourth, no stable solutions can be found for sufficiently large  $\mathbf{w}$  and  $a$ .

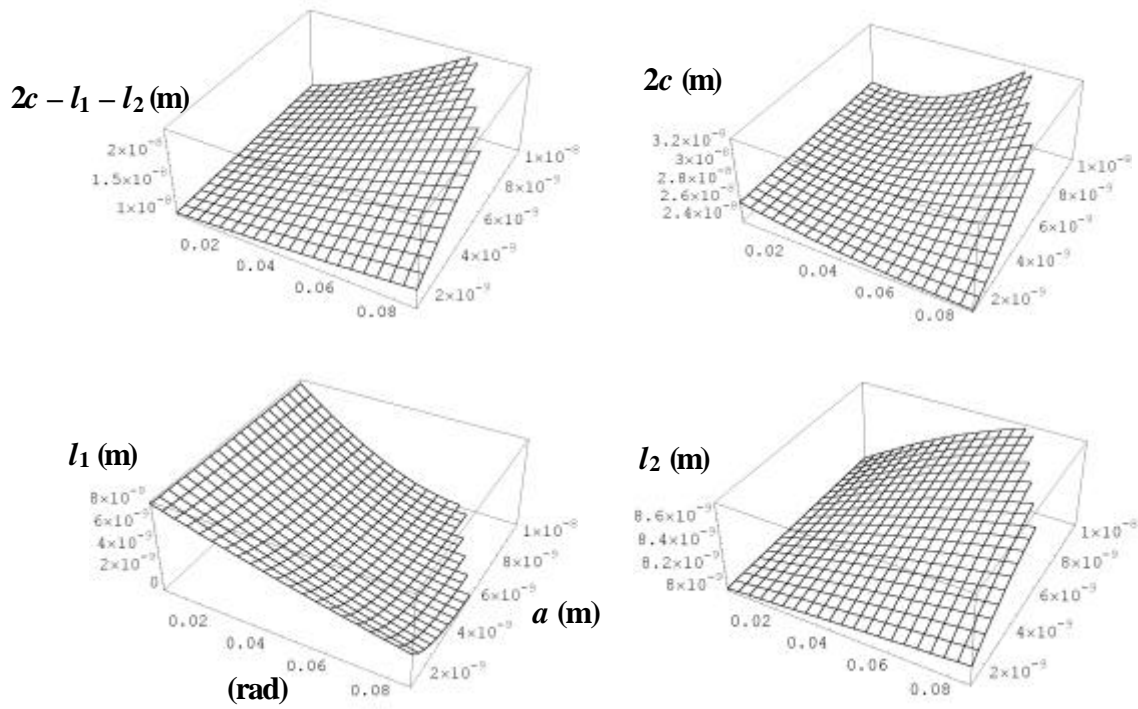


**Figure 3:** Dependence of the traction-free zone length, the total crack length, and the lengths of the cohesive zones at the crack head and crack tip on the dislocation dipole strength and arm length.

### Comparison of Cohesive and Elastic Cracks

Figure 4 compares the traction-free zone lengths of Zener-Barenblatt cracks to the crack lengths of elastic Zener cracks. The conclusion is that for the nanocracks considered here (with small crack head opening  $b_T = 4_{cr}$ ) a significant discrepancy exists between the two predictions. The predicted elastic cracks are significantly longer than the predicted traction-free zones. Also, the discrepancy increases as  $\mathbf{w}$  and  $a$  decrease in magnitude.

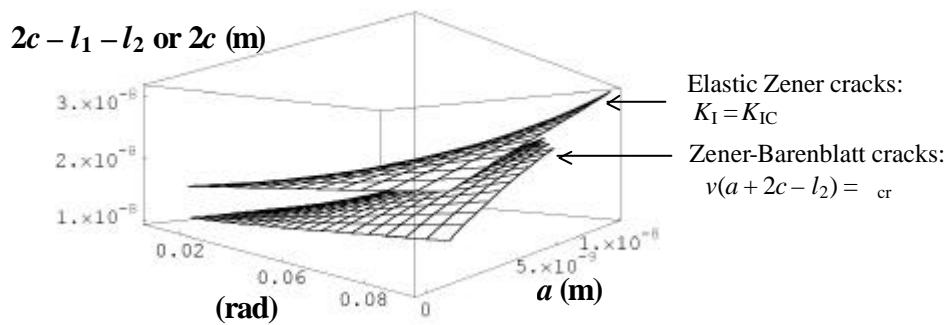


**Figure 4:** Comparison of the traction-free zone lengths of Zener-Barenblatt cracks with the lengths of elastic Zener cracks.

### Dependence of Crack Lengths on Material

Figure 5 compares the traction-free zone lengths and the total lengths of cohesive cracks in various metals. The lengths of elastic cracks are also plotted in the figure. All lengths are plotted against the cohesive strengths  $\mathcal{S}_c = 2g_{cr} = gb$  of the metals. In all cases,  $w = 1^\circ$  and  $2a = 4$  nm. The results show that the various lengths do not have a clear correlation with  $\mathcal{S}_c$ . Similarly, no clear correlation is found when they are plotted against  $g$ ,  $G$  or  $K_{IC}$ . In contrast, the length of an elastic Zener crack subjected to the opening  $b_T$  (no disclination loading) varies monotonically with the material parameters. The figure also shows that the predicted length of a disclinated elastic crack overestimates the traction-free zone length of the cohesive crack but underestimates the total length of the cohesive crack.

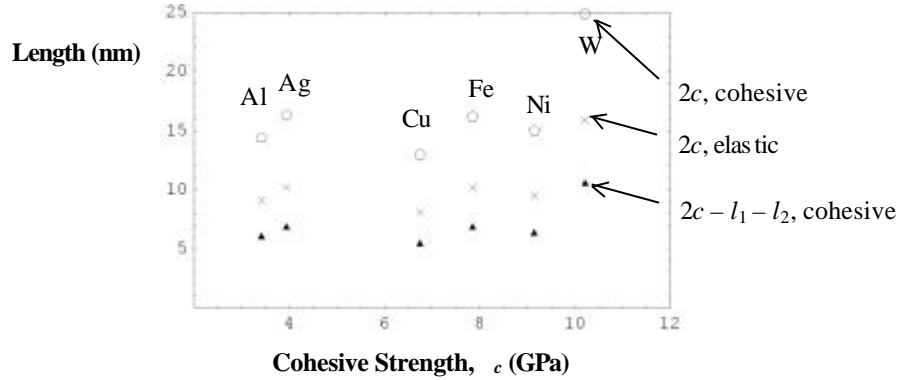


**Figure 5:** Comparison of the total crack lengths (pentagons), the traction-free zone lengths (triangles) of cohesive cracks, and the crack lengths (crosses) of elastic cracks.

#### 4. SUMMARY

The equilibrium length of a stable mode I Zener-Barenblatt crack subjected to the loading of a disclination dipole is investigated in this paper. The crack length solutions are obtained by the method of dislocation modeling of the entire cohesive crack. Exact expressions constructed from the crack opening displacement and the consistency relations are solved numerically for the total crack length and the cohesive zone lengths. For small crack head opening displacement of the order of nanometers, numerical results indicate that: (i) the cohesive zones constitute a significant portion of the total crack, (ii) the elastic crack length, while significantly larger than the traction-free zone length, is significantly smaller than the total cohesive crack length, (iii) the traction-free zone length increases with the disclination dipole strength and the dipole arm length, and (iv) the cohesive zone at the crack head decreases in size with the disclination parameters, while that at the crack tip increases in size with these parameters.

#### REFERENCES

1. Müllner, P. and Kuschke, W.-M. (1997). *Scrip. Mater.* 36, 1451.
2. Müllner, P. (1997). *Mater. Sci. Engng.* A234-236, 94.
3. Wu, M. S. (2001). *Int. J. Engng. Sci.*, accepted.
4. Pearson, W. B. (1967). *Handbook of Lattice Spacings and Structures of Metals*, Vol. 2. Pergamon Press, Oxford.
5. Hirth, J. (1982). *Theory of Dislocations*, Second Edition. Krieger Publishing Company, Malabar.